CCFE
CULHAM CENTRE FOR FUSION ENERGY

CCFE-PR(15)115

D.M. Harting, S. Wiesen, M. Groth, S. Brezinsek, G. Corrigan,
G. Arnoux, P. Boerner, S. Devaux, J. Flanagan, A. Järvinen,
S. Marsen, D. Reiter and JET EFDA contributors

Intra-ELM Phase Modelling of a JET ITER-like Wall H-mode Discharge with EDGE2D-EIRENE

Intra-ELM Phase Modelling of a JET ITER-like Wall H-mode Discharge with EDGE2D-EIRENE

D.M. Harting[1], S. Wiesen[2], M. Groth[3], S. Brezinsek[2], G. Corrigan[1], G. Arnoux[1], P. Boerner[2], S. Devaux[1], J. Flanagan[1], A. Järvinen[1], S. Marsen[1], D. Reiter[1] and JET EFDA contributors

[1]EURATOM-CCFE Fusion Association, Culham Science Centre, OX14 3DB, Abingdon, OXON, UK
[2]Institute of Energy and Climate Research – IEK4, Association EURATOM-FZJ, D-52425 Jülich, Germany
[3]Aalto University, Association EURATOM-Tekes,Espoo, Finland
[4]Max-Planck-Institut für Plasmaphysik, EURATOM-Assoziation, D-17491 Greifswald, Germany

ABSTRACT

We present the application of an improved EDGE2D-EIRENE SOL transport model for the ELM phase utilizing kinetic correction of the sheath-heat-transmission coefficients and heat-flux-limiting factors used in fluid SOL modelling. With a statistical analysis over a range of similar Type-I ELMy H-mode discharges performed at the end of the first JET ITER-like wall campaign, we achieved a fast ($\Delta t = 200\mu s$) temporal evolution of the outer midplane n_e and T_e profiles and the target-heat and particle-flux profiles, which provides a good experimental data set to understand the characteristics of an ELM cycle. We will demonstrate that these kinetic corrections increase the simulated heat-flux-rise time at the targets to experimentally observed times but will not affect the still by the simulations underestimated power-decay time at the target. This longer decay times are potentially related to a change of the local recycling coefficient at the tungsten target plate directly after the heat pulse.

1. INTRODUCTION

Previous modelling of the full JET ELM cycle [1] in JET equipped with carbon walls (JET-C) has shown that the fluid approximation for the parallel transport in EDGE2D-EIRENE [2] [3] is sufficient to reproduce the energy balance in terms of the ELM-wetted area and power in-out asymmetry. However, the peak-power load q_{max} obtained in the intra-ELM phase of those simulations was overestimated leading to a factor of 8 higher value of qmax compared to the experiment while the power-decay time at the target was underestimated. This resulted in total integrated target-energy densities similar to those observed experimentally (and thus reproduced the characteristics of a free streaming approximation of ELM filamentary transport as proposed in [4]) but the time-wise evolution of q_{max} at the target still suffered from the assumption of the parallel scrape-off layer (SOL) transport being classical in the fluid simulations.

In fact, 1D kinetic simulation for a typical type-I ELMy JET SOL [5] have shown that within the intra-ELM phase, the fluid approximation for parallel transport in the SOL breaks down and kinetic effects play a significant role for the heat flux transported towards the target plate. It is specifically the electron-heat channel, which is strongly overestimated when using a classical fluid treatment for the parallel transport.

We present the results of the application of an improved EDGE2D-EIRENE SOL transport model for the intra-ELM phase of discharges from a two-week lasting JET ITER-like wall [6] (ILW) operation. A type-I ELMy H-mode low-triangular neutral-beam heated tokamak discharges (I_p/B_t = 2.0MA/2.0T, P_{NBI} = 12MW) in low triangularity had been continuously repeated to obtain a footprint of the material migration under quasi steady-state wall conditions prior to the removal of plasma-facing components for further analysis [7]. This group of discharges provides an unprecedented data set to statistically analyse the intra-ELM evolution of pedestal and target plasma profiles experimentally.

The derived time-dependent kinetic correction factors (KF) from [5], i.e. sheath-heat transmission-coefficients and kinetic heat-flux limiters are applied for simulations of the ELM phase of the

aforementioned discharges. The sensitivity of the simulations on the kinetic effects is studied in order to match the experimentally observed ELM peak power-loads and decay times derived from infrared thermography. The resulting more realistic ELM background plasma configurations (in the scope of 2D fluid SOL simulations) will be used further for material migration studies and tungsten source and transport analysis employing dedicated plasma-surface interaction codes such as WallDYN [8] and ERO [9].

2. STATISTICAL ELM ANALYSIS

The previous modelling of the ELM crash [1] was compared to experimental data of Pulse No: 73569 from JET-C. Later in [10] it was reported however that in JET-ILW the ELM duration can be much longer than in JET-C, but the same signature can be recovered at same pedestal temperature. ELMs with long duration are also present in the discharges we analyse here: Figure 1 shows the pedestal drop after the ELM crash for the previously modelled Pulse No: 73569 from JET-C and one of the ILW discharges analysed in this paper. The time resolution of the edge Interferometer channel for the density measurement has significantly improved after the JET-C campaigns, which allows the estimation of the density pedestal drop time for the JET-ILW Pulse No: 83559. But the fast drop in edge electron temperature measured by the edge ECE channel and in the stored energy measurement indicates ELM durations below the temporal resolution of the measurement (<400μs). For the ILW discharge, the drop of the pedestal density and temperature extends over a much longer range of 4-5ms after the ELM crash, which was not anticipated before the installation of the JET-ILW.

2.1 OUTER MIDPLANE PLASMA PROFILES

The high resolution Thomson scattering (HRTS) diagnostic at the outer midplane (OMP) of JET can measure every 50ms radial n_e and T_e profiles. This frequency is much too slow to resolve the evolution of the density and temperature pedestal during an ELM. To obtain an evolution of n_e and T_e profiles with a time resolution of $\Delta t = 200\mu s$, we extracted the HRTS measurements relative to the ELM trigger, for which we used the integrated inner target WI-emission from physical sputtering. For the statistical analysis we used 53 similar discharges from the range Pulse No's: 83628 – 83727 and averaged 20-50 individual HRTS measurements in a time window of $\Delta t = 200\mu s$ (averaging out also any filamentary structures). We restricted the statistical analysis to times between 10.0s and 14.0s of the discharge with an average ELM frequency of $f_{ELM} \approx 30Hz$. In our statistical analysis only ELMs which had an ELM-free time of $\Delta t = 20ms$ before and after the ELM. The profiles from the statistical analysis of the HRTS measurements for dedicated times points after the ELM trigger ($t = 0$ corresponds to the last OMP profile, unaffected by the ELM) are shown in Figure 2, defining different phases of the time evolution of the OMP profiles.

Electron density profile evolution at the OMP:

Phase 1: The electron density at the top of the pedestal drops quickly in the first 0.4ms after

the ELM crash (green curve) by 25%. In this first 0.4ms the particles are flushed into the SOL, where the density increases from 1x1019m-3 to ~$2.5 \times 10^{19} m^{-3}$

Phase 2: From 0.4ms to ~1.6ms (blue curve) the density stays about constant in the SOL, but is still dropping slightly up to 10cm inside of the separatrix.

Phase 3: After 1.6ms the density drops further in the SOL up to 2.5cm inside of the separatrix to its lowest profile around ~5.2ms (pink).

Phase 4: After 5.2ms, the density recovers to its initial pre-ELM profile until the next ELM is triggered.

Electron temperature profile evolution at the OMP:

Phase 1: In the first 0.4ms some of the pedestal heat is flushed into the SOL.

Phase 2: After 0.4ms the electron temperature drops steady going until ~1.2ms to its lowest profile (blue).

Phase 3: From 1.2ms to ~2.8ms the electron temperature stays then roughly constant.

Phase 4: After 2.8ms the electron temperature pedestal starts recovering.

This behaviour can also be observed in the evolution of the relative pedestal density and temperature drops ($\Delta n_e/n_e$, $\Delta T_e/T_e$) shown in Figure 3.

2.2 OUTER TARGET HEAT AND PARTICLE FLUX PROFILES

Due to a high time resolution of the measurements for the heat flux by the infrared camera (IR) and the particle flux measured by Langmuir probes at the outer target (OT) we only needed to extract and average profiles relative to the ELM crash in the statistical analysis from one discharge (#83562) to achieve a sufficient number of individual measurements in each time window (Figure 4). The heat flux at the outer target peaks quickly at 0.6ms before it slowly decays until ~5ms. The particle flux starts rising at the same time as the heat flux but has a delayed peak at ~1.2ms before it decays slowly until ~5-6ms. A strong second peak in the particle flux can be observed around 8ms. The origin of this second peak in the particle flux is currently not clear, but is potentially related to flux amplification at the target plate at that time.

3. SIMULATION OF THE INTRA-ELM PHASE

In order to simulate the intra-ELM phase with the EDGE2D-EIRENE code, we first simulated pure deuterium (no impurities) steady-state pre-ELM conditions. We used 10.5MW of input power entering the simulation domain from the core (uniformly distributed between electrons and ions) and setup a transport barrier by dropping the anomalous perpendicular transport coefficients in the first few centimetres inside of the separatrix to $\chi_e = \chi_i = 0.5 m^2 s^{-1}$ for the electron and ion perpendicular heat conductivity and to $D = 0.04 m^2 s^{-1}$ for the perpendicular particle diffusivity. The transport barrier for the particles is also extended 1.5cm in to the SOL, to match the experimental

pre-ELM OMP density profiles. The OMP separatrix density $n_{sep,OMP} = 2.4x10^{19}m^{-3}$ is achieved by a fixed injection rate and we used default heat-flux limiting factors [11] for electrons and ions of $\alpha_{0e} = \alpha_{0i} = 0.2$. The sheath heat transmission factors were set in the pre-ELM phase to $\gamma_e = 2.5$ and $\gamma_i = 4.5$ for electrons and ions respectively.

We implemented the kinetic corrections factors (KF) proposed in [5] by using the formulas for the sheath-heat-transmission factors described in the paper and the following parameterization for the flux-limiting factors: For the electron heat-flux limiting factor we used a double exponential decay up to 100µs and then an exponential increase up to 560µs where pre-ELM values of the electron heat-flux-limiting factors were reached again. The ion-heat-flux limiting factors were multiplied by 3 compared to pre-ELM values for times up to 40µs. After that we applied an exponential decay up to 200µs and again an exponential increase up to 560µs where the pre-ELM value of the ion-heat-flux limiting factor was reached again. The implemented KF are shown in Figure 5 where the heat-flux- limiting factors were normalized to its pre-ELM values α_{0e} and α_{0i}.

Similar to [1] the ELM model in EDGE2D-EIRENE allows specifying a radial profile of modified perpendicular transport coefficient for a selected duration ΔtELM of the ELM. Here we chose a triangular spatial shape peaking at or slightly inside of the separatrix with a radial extend at the OMP of 7cm inside of the separatrix and 1cm outside into the SOL. Beyond this region, the perpendicular diffusivities and conductivities were set to $1m^2s^{-1}$. We investigated three different ELM durations of $\Delta t_{ELM} = 200\mu s$, 1ms and 3ms. The corresponding peak transport coefficients of the spatial triangular shape are listed in Table 1 together with the achieved ELM energies ΔEELM. The first line of Table 1 lists the corresponding experimental values. The experimental ELM energy was estimated here in two ways. With the assumption of $T_i = T_e$ we calculated from the averaged experimental OMP ne and Te profiles the stored energy and estimated an ELM energy of 120kJ. By applying the same statistical analysis as described above for the measured diamagnetic energy WDIA, we estimated an average ELM energy of 160kJ, which suggest an experimental ELM energy in the range of 120–160kJ.

By applying a very short ELM duration of $\Delta t_{ELM} = 200\mu s$ (as used in previous ELM simulations [1]) we underestimate the pedestal drop times at the OMP for the electron density ($t_{drop,ne}$) and Temperature ($t_{drop,Te}$) as well as the rise ($t_{peak,Q}$) and the decay ($t_{decay,Q}$) times of the heat flux at the OT dramatically (see Table 1). By applying the kinetic correction factors (KF) proposed in [5], we can increase the rise and decay times of the heat flux at the OT by 0.1ms, but this is still not enough to get to the experimental raise time of 1.2ms. Also the peak-power load is reduced nearly by a factor of two, while applying the KF (Figure 6). The spreading of the heat load over a larger time window is mainly attributed to the strong limitation of the electron heat flux. The additional pre-peak observed in the heat load at 4µs while applying the KF is a combination effect of the reduced electron heat flux limit and the strongly increased electron sheath heat transmission factor at that time.

By increasing the ELM duration to $\Delta t_{ELM} = 1ms$, we can achieve an electron temperature pedestal

drop time similar to the experimental drop time of 1ms but a slightly too long density pedestal drop time of 0.75ms. Also the raise and decay times of the heat flux are still too short. By applying the KF to the 1ms ELM duration simulation, we can nearly achieve the experimental density pedestal drop time and OT heat flux rise time. The heat-flux decay time at the OT is unaffected by the KF. If we further increase the ELM duration to $\Delta t_{ELM} = 3$ms, we can match the decay time of the heat flux, but the pedestal drop times are much too long compared to the experimental pedestal drop times. Also in this case, if we apply the KF, we can increase the heat flux raise time from 0.35ms to 0.5ms, which is very close to the experimentally observed 0.56ms.

DISCUSSION AND CONCLUSION

From the experimental OMP electron density and temperature profiles in Figure 2 we can conclude, that we have a short (400μs) ELM event (MHD), which drops the pedestal density by 25%, destroys the transport barrier and flushes particles and heat into the SOL. The electron temperature profiles continue then to drop steady going until 1.2ms while the density profile stays roughly constant until 1.6ms (with a slight decrease in the first 10cm inside of the separatrix). After 1.6ms the fuelling of the plasma is reduced until ≈5.2ms, which reduces the SOL density up to 2.5cm inside of the separatrix. The reduced fuelling of the plasma between 1.6ms and 5.2ms must be associated with a transient particle pump during this period. As the fuelling of the plasma is determined by the recycling at the target plates and not the deuterium injection, it is likely that temporary the recycling coefficient at the target plate is reduced representing a sink for the plasma. The temperature profile on the other hand stays roughly constant between 1.2ms and 2.8ms and starts recovering at 3-4ms, which suggests that the transport barrier re-establishes around that time.

The simple ELM model available in EDGE2D-EIRENE cannot reproduce this complex behaviour during the ELM cycle at the moment. But we could demonstrate that the inclusion of kinetic corrections to the heat flux limits (proposed in [5]) can reproduce the pedestal drop times $t_{drop,Te}$ and $t_{drop,ne}$, as well as the rise time $t_{peak,Q}$ of the heat flux at the outer target. We suggest extending the current ELM model in EDGE2D-EIRENE by a second phase (after the first 400μs) where only L-mode like transport coefficients are applied and an additional particle pump at the target plate would account for the reduced pedestal fuelling before the transport barrier (around 3-4ms) has been re-established. This could potentially reproduce the long decay times of the heat flux observed experimentally together with the fast drop (400μs) of the density pedestal.

ACKNOWLEDGMENTS

This project has received funding from the European Union's Horizon 2020 research and innovation programme under grant agreement number 633053 and from the RCUK Energy Programme [grant number EP/I501045]. The views and opinions expressed herein do not necessarily reflect those of the European Commission..

REFERENCES

[1]. S. Wiesen et al., Plasma Physics and Controlled Fusion **53** (2011) 124039

[2]. R. Simonini, G. Corrigan, et al., Contribution to Plasma Physics **34** (1994) 368–373

[3]. S. Wiesen, http://www.eirene.de/e2deir_report_30jun06.pdf

[4]. W. Fundamenski and R.A. Pitts et al., Plasma Physics and Controlled Fusion **48** 109 (2006)

[5]. D. Tskhakaya et al., Contribution to Plasma Physics **48**, No.1-3, 89-93 (2008)

[6]. G.F. Matthews et al., Physica Scripta **2011** (2011) 014001.

[7]. S. Brezinsek et al., Nuclear Fusion **53** 083023 (2013)

[8] K. Schmid et al., Journal of Nuclear Materials **415** (2011) 284

[9] A. Kirschner et al., Nuclear Fusion **40**, No.5 (2000) 989

[10]. B. Siegling et al., Plasma Physics and Controlled Fusion **55** (2013) 124039

[11]. P.C. Stangeby, "The Plasma Boundary of Magnetic Fusion Devices", IOP Publishing Ltd, Bristol UK, 2000

Case	E_{ELM} [kJ]	D_{ELM} [m^2/s]	$\chi_{e,ELM}$ [m^2/s]	$\chi_{i,ELM}$ [m^2/s]	$t_{drop,Te}$ [ms]	$t_{drop,ne}$ [ms]	$t_{peak,Q}$ [ms]	$t_{decay,Q}$ [ms]
Exp.	120 - 160	-	-	-	1.2	0.4	0.56	4
t_{ELM} = 0.2ms no KF	97	200	100	300	0.2	0.2	0.09	0.64
t_{ELM} = 0.2ms with KF	92	200	100	300	0.2	0.2	0.14	0.76
t_{ELM} = 1.0ms no KF	125	10	30	30	1.0	0.75	0.3	1.53
t_{ELM} = 1.0ms with KF	124	10	30	30	1.0	0.5	0.46	1.53
t_{ELM} = 3.0ms noKF	156	10	6	6	3.0	2.2	0.35	3.65
t_{ELM} = 3.0ms with KF	155	10	6	6	3.0	2.2	0.5	3.65

Table 1: Overview of the experimental and simulated ELM parameters including ELM energy ΔE_{ELM}, peak value of perpendicular transport coefficients during the ELM, the pedestal drop times of n_e ($t_{drop,ne}$) and T_e ($t_{drop,Te}$), and the raise ($t_{peak,Q}$) and decay ($t_{decay,Q}$) times of the heat flux at the outer target.

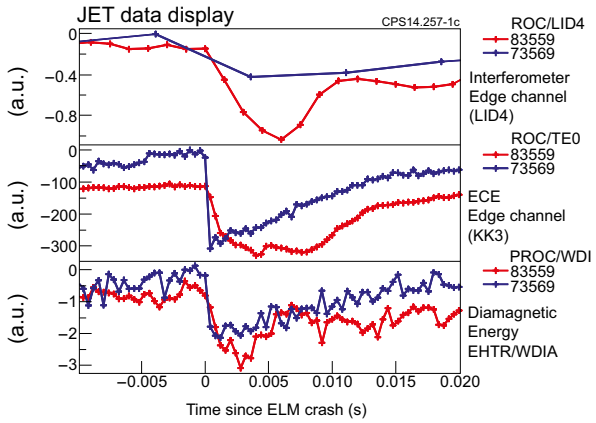

Figure 1: Drop of the pedestal density (top graph), electron temperature (middle graph) and stored energy (bottom graph) after the ELM crash for the previously modelled JET-C Pulse No: 73569 (blue curves) and the JET-ILW Pulse No: 83559 (red curves).

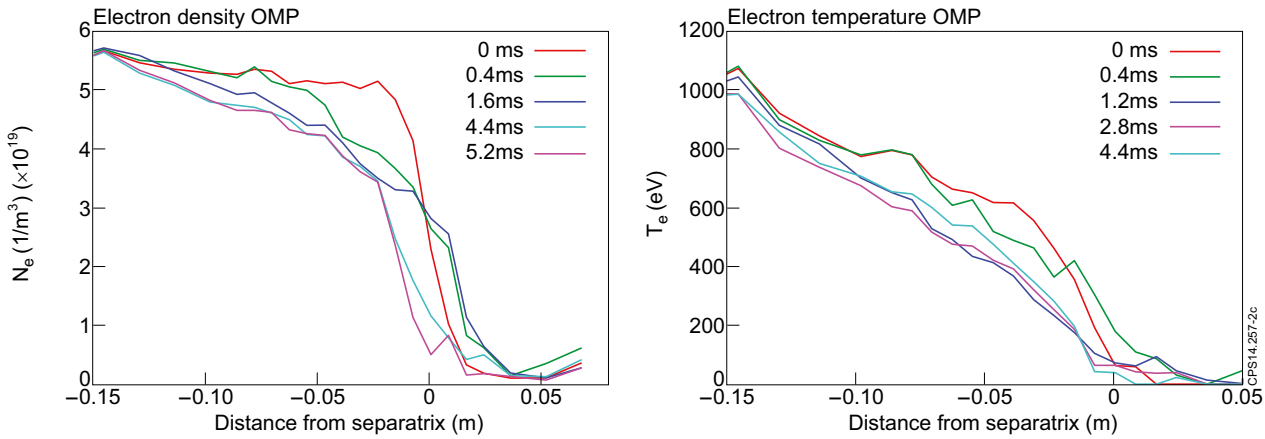

Figure 2: Averaged OMP electron density and temperature profiles from the statistical analysis of the HRTS data for characteristic time points after the ELM crash.

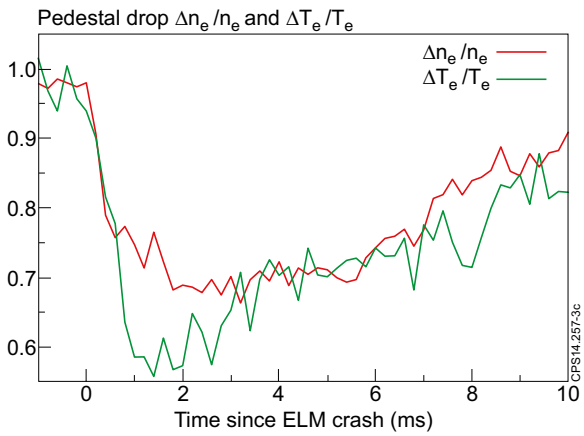

Figure 3: Temporal evolution of the relative pedestal drops at the OMP of the electron density (2.5cm inside of separatrix) and temperature (3.3cm inside of separatrix).

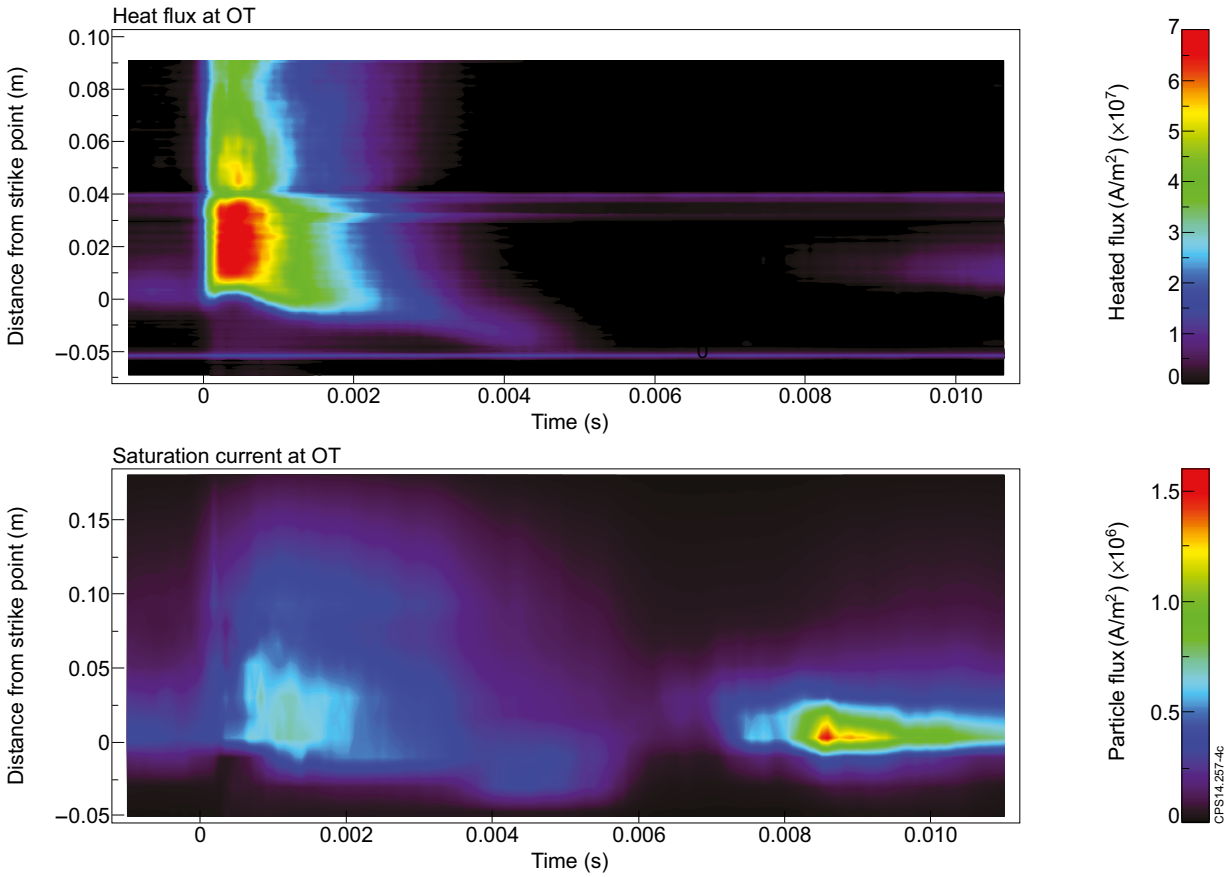

Figure 4: Averaged heat and particle flux profiles at the OT from the statistical analysis.

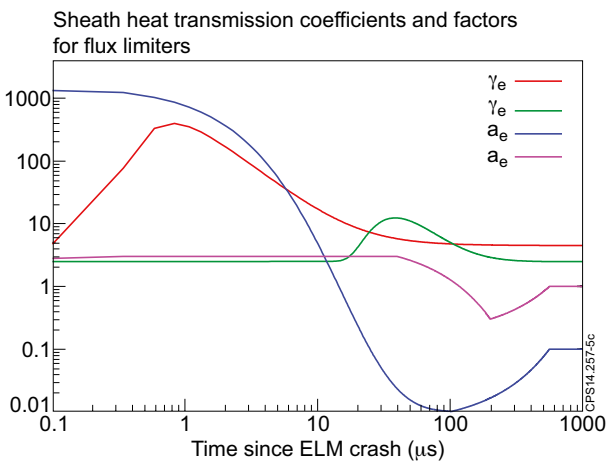

Figure 5: Sheath heat transmission coefficients γ_i, γ_e and heat flux limiting factors α_i, α_e normalized to pre ELM values α_{0e}, α_{0i}.

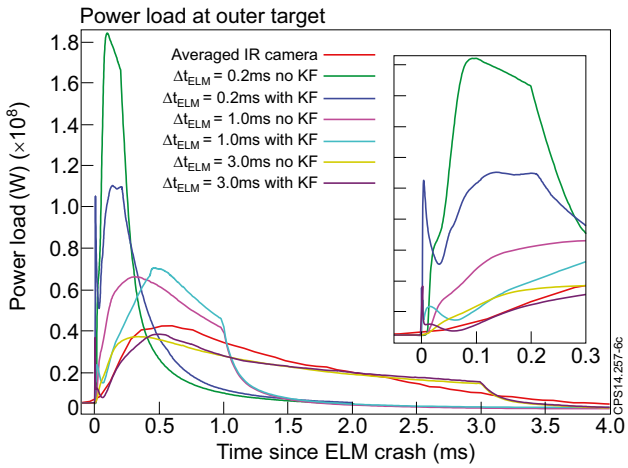

Figure 6: Comparison of the temporal evolution of the integrated power load on the OT between IR measurement and different ELM durations in the simulations. The second graph inside the first one is a zoom in to the region between t = –0.05ms and 0.3ms to illustrate the pre peak in heat flux originated from the KF